Обзор arXiv/astro-ph, 1-10 сентября 2019

От Сильченко О.К.

ArXiv: 1909.01344

Galaxy disc scaling relations: A tight linear galaxy–halo connection challenges abundance matching

Lorenzo Posti[1,⋆], Antonino Marasco[2,3], Filippo Fraternali[2], and Benoit Famaey[1]

[1] Université de Strasbourg, CNRS UMR 7550, Observatoire astronomique de Strasbourg, 11 rue de l'Université, 67000 Strasbourg, France.
[2] Kapteyn Astronomical Institute, University of Groningen, P.O. Box 800, 9700 AV Groningen, the Netherlands
[3] ASTRON, Netherlands Institute for Radio Astronomy, Oude Hoogeveensedijk 4, 7991 PD, Dwingeloo, The Netherlands

Received XXX; accepted YYY

ABSTRACT

In ΛCDM cosmology, to first order, galaxies form out of the cooling of baryons within the virial radius of their dark matter halo. The fractions of mass and angular momentum retained in the baryonic and stellar components of disc galaxies put strong constraints on our understanding of galaxy formation. In this work, we derive the fraction of angular momentum retained in the stellar component of spirals, f_j, the global star formation efficiency f_M, and the ratio of the asymptotic circular velocity ($V_{\rm flat}$) to the virial velocity f_V, and their scatter, by fitting simultaneously the observed stellar mass-velocity (Tully-Fisher), size-mass, and mass-angular momentum (Fall) relations. We compare the goodness of fit of three models: (i) where the logarithm of f_j, f_M, and f_V vary linearly with the logarithm of the observable $V_{\rm flat}$; (ii) where these values vary as a double power law; and (iii) where these values also vary as a double power law but with a prior imposed on f_M such that it follows the expectations from widely used abundance matching models. We conclude that the scatter in these fractions is particularly small ($\sim$ 0.07 dex) and that the "linear" model is by far statistically preferred to that with abundance matching priors. This indicates that the fundamental galaxy formation parameters are small-scatter single-slope monotonic functions of mass, instead of being complicated non-monotonic functions. This incidentally confirms that the most massive spiral galaxies should have turned nearly all the baryons associated with their haloes into stars. We call this the failed feedback problem.

Key words. galaxies: kinematics and dynamics – galaxies: spiral – galaxies: structure – galaxies: formation

Масштабные соотношения

Δ times the critical density of the Universe. Haloes, then, adhere to the following scaling laws (e.g. Mo et al. 2010):

$$M_{\rm h} = \frac{1}{GH}\sqrt{\frac{2}{\Delta}}V_{\rm h}^3; \tag{3}$$

$$R_{\rm h} = \frac{1}{H}\sqrt{\frac{2}{\Delta}}V_{\rm h}; \tag{4}$$

$$j_{\rm h} = \frac{2\lambda}{H\sqrt{\Delta}}V_{\rm h}^2, \tag{5}$$

where G is the gravitational constant and $\lambda = j_{\rm h}/\sqrt{2}R_{\rm h}V_{\rm h}$ is the halo spin parameter, as in the definition by Bullock et al. (2001, which is conceptually equivalent to the classic definition in Peebles 1969). The distribution of λ for ΛCDM haloes is very well studied and it is known to have a nearly log-normal shape – with mean $\log\overline{\lambda} \approx -1.456$ and scatter $\sigma_{\log\lambda} \approx 0.22$ dex – irrespective of halo mass. Henceforth, since λ is not a function of $V_{\rm h}$, Eq. (5) is a simple power law $j_{\rm h} \propto V_{\rm h}^2$, while also Eq. (3)-(4) are obviously similar power laws.

3.2. Galaxy formation parameters

We very simply parametrise the intrinsically complex processes of galaxy formation, by considering that, to first order, galaxies form out of the cooling of baryons within the virial radius of their halo. The fundamental parameters we consider are then the following fractions:

$$f_M \equiv \frac{M_\star}{M_{\rm h}}; \qquad f_j \equiv \frac{j_\star}{j_{\rm h}}; \qquad f_V \equiv \frac{V_{\rm flat}}{V_{\rm h}}; \qquad f_R \equiv \frac{R_{\rm d}}{R_{\rm h}}. \tag{6}$$

pendent. It is easy to work out their relation as a function of the dark matter halo profile, which turns out to be analytic in the case of an exponential disc with a flat rotation curve (see Appendix A), i.e.,

$$f_R = \frac{\lambda}{\sqrt{2}}\frac{f_j}{f_V}. \tag{7}$$

An analogous result was already derived analytically by Fall (1983). For more realistic haloes, for example a Navarro et al. (1996, NFW) halo, a similar proportionality still exists, and can be worked out with an iterative procedure (see e.g. Mo et al. 1998).

With these definitions we can rewrite the dark matter relations of Eqs. (3)-(5) now for the stellar discs as

$$M_\star = \frac{f_M}{GH}\sqrt{\frac{2}{\Delta}}\left(\frac{V_{\rm flat}}{f_V}\right)^3; \tag{8}$$

$$R_{\rm d} = \frac{\lambda f_j}{H\sqrt{\Delta}}\frac{V_{\rm flat}}{f_V^2}; \tag{9}$$

$$j_\star = \frac{2\lambda f_j}{H\sqrt{\Delta}}\left(\frac{V_{\rm flat}}{f_V}\right)^2. \tag{10}$$

Аналитические модели

Первая, самая простая

$$\log f = \alpha \log V_{\rm flat}/{\rm km\,s^{-1}} + \log f_0. \quad (11)$$

Thus, we have a slope (α) and a normalisation (f_0) for each of the three fractions f_M, f_j, and f_V. In this case, we adopt uninformative priors for all the free parameters.

(ii) The second model assumes a more complicated double power-law dependence of f on $V_{\rm flat}$,

$$f = f_0 \left(\frac{V_{\rm flat}}{V_0}\right)^{\alpha} \left(1 + \frac{V_{\rm flat}}{V_0}\right)^{\beta-\alpha}. \quad (12)$$

We have two slopes (α, β) and a normalisation (f_0) that are different for each of the three f; while the scale velocity (V_0), which defines the transition between the two power-law regimes, is the same for the three fractions for computational simplicity. Also in this case, we use uninformative priors for all the free parameters.

(iii) The last model has the same functional form as model (ii), i.e. Eq. (12), with uninformative priors for f_j and f_V; while we impose normal priors on the slopes (α, β), normalisation (f_0) and scale velocity (V_0) such that the global star formation efficiency follows the results of the abundance matching model by M+13. In order to properly account for the sharp maximum of f_M at $M_{\rm h} \approx 4 \times 10^{11} M_{\odot}$, we slightly modify the functional form of $f_M = f_M(V_{\rm flat})$ as

$$f_M = f_0 \left(\frac{V_{\rm flat}}{V_0}\right)^{\alpha} \left[1 + \left(\frac{V_{\rm flat}}{V_0}\right)^{\gamma}\right]^{\beta-\alpha}, \quad (13)$$

where $\gamma = 3$ since $M_{\rm h} \propto V_{\rm flat}^3$.

Что «лежит» под 3й моделью:

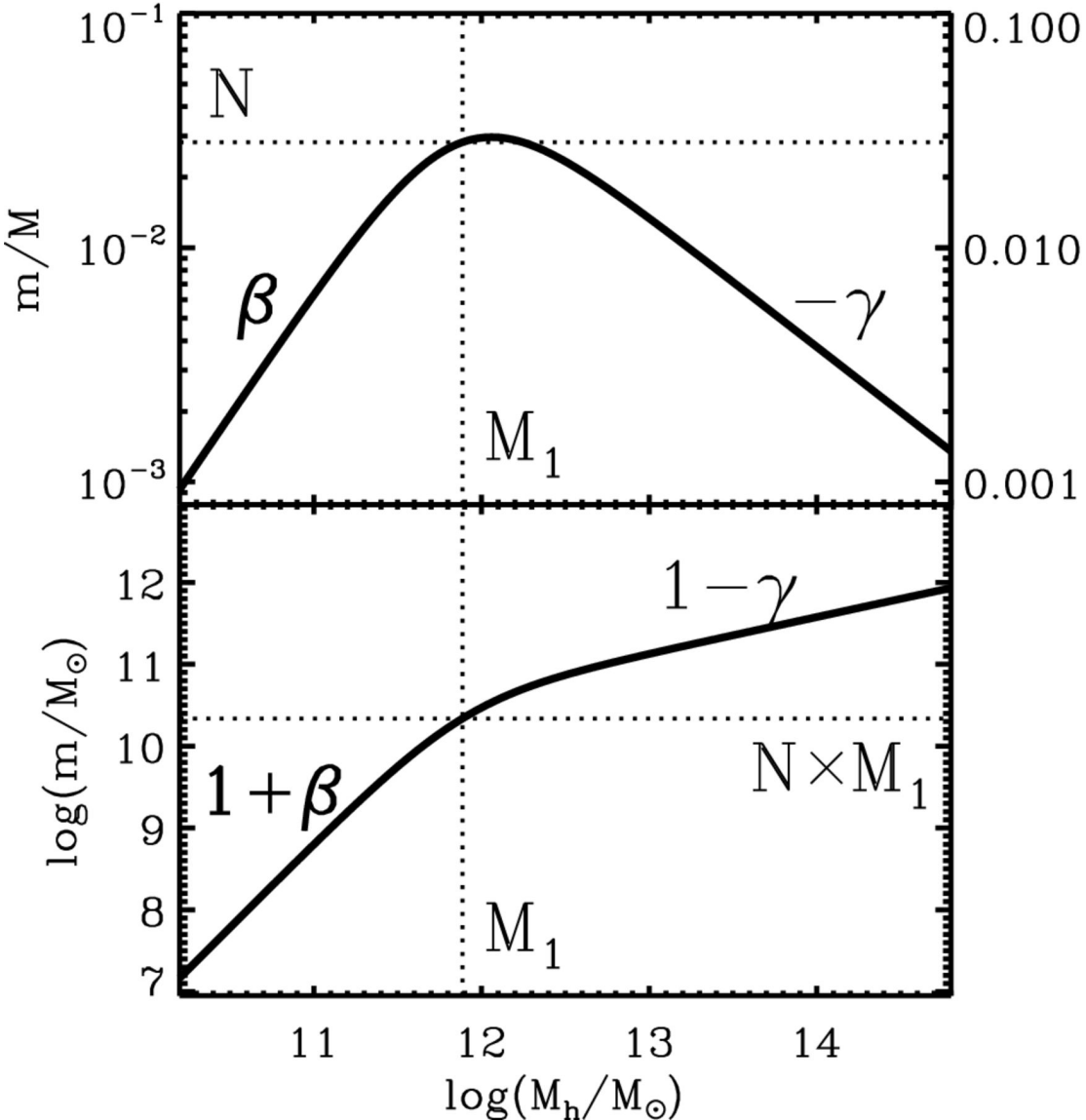

Moster+2013

Что это значит для связи «гало-звезды»:

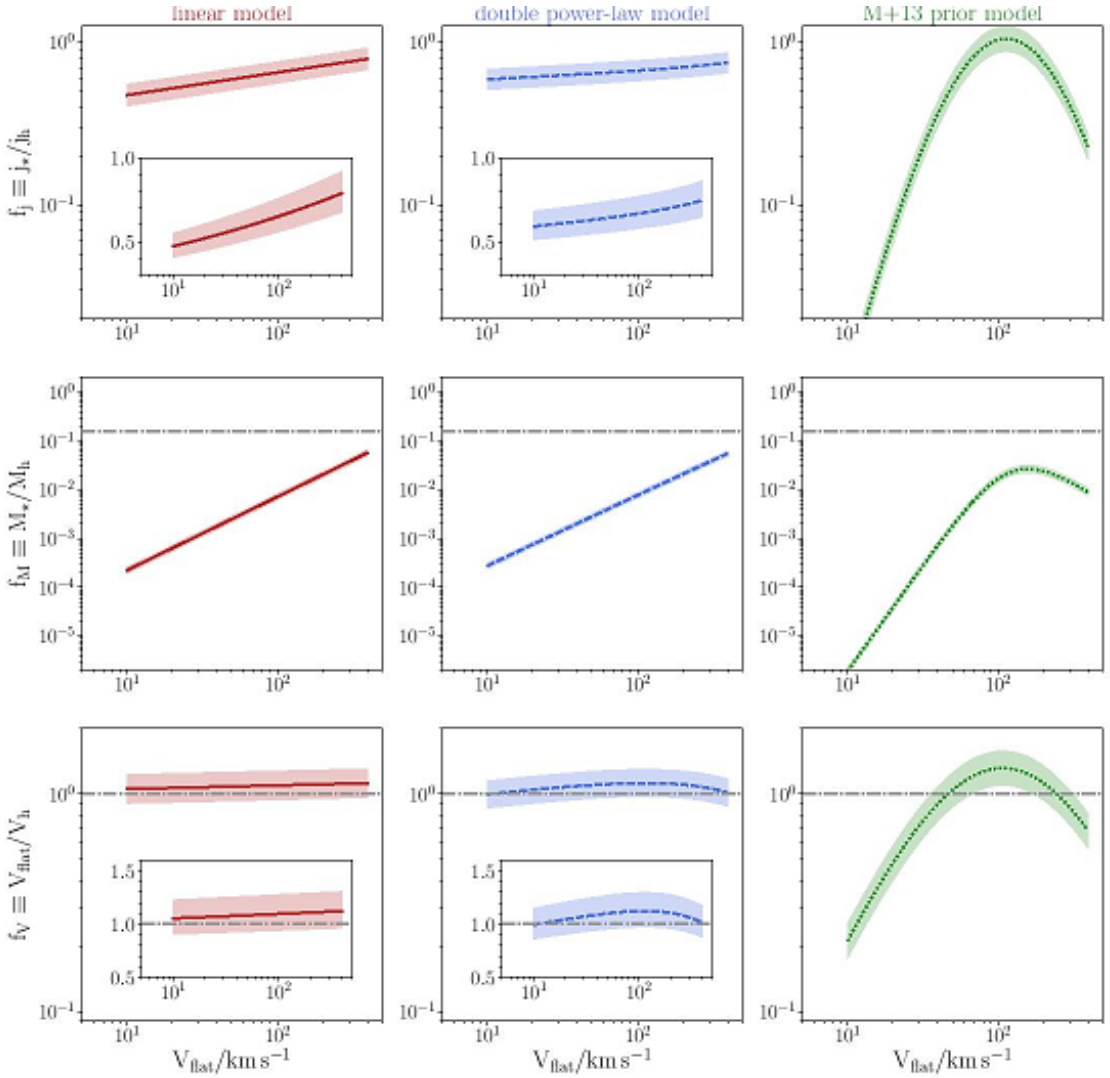

Fig. 3. Model predictions. We show how f_j (top row), f_M (middle row), and f_V (bottom rows) vary as a function of V_{flat} for the three best models (columns). In the middle row the dot-dashed line shows the value of the cosmic baryon fraction $f_b = 0.157$, while in the bottom row the dot-dashed line indicates the value $f_V = 1$. The insets show a zoom-in of the plots in linear scale.

Наблюдения: SPARC+LittleTHING

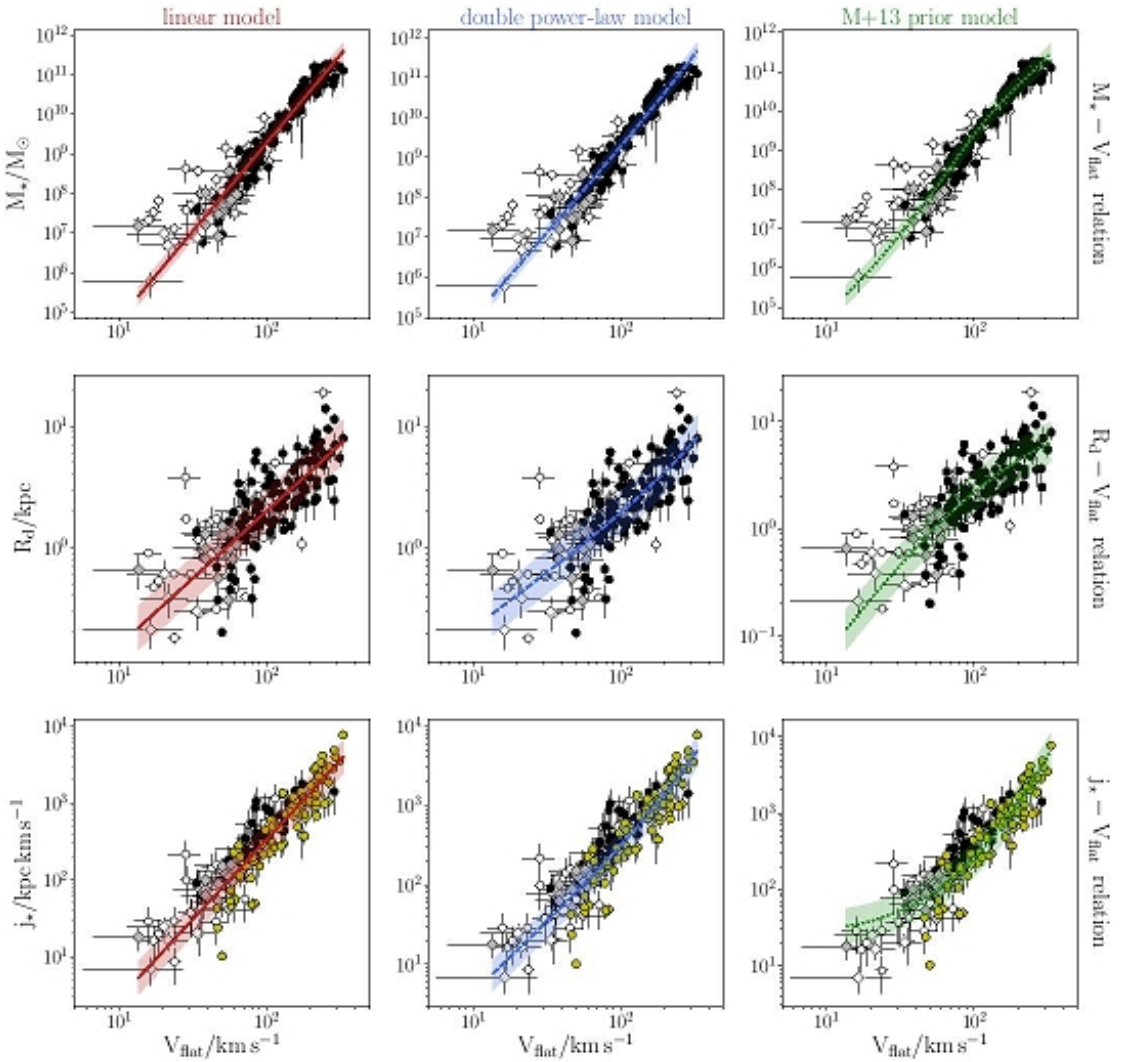

Fig. 2. Comparison of the three best models obtained with different assumptions on f_j, f_M, and f_V with the data from SPARC galaxies (circles) and LITTLE THINGS galaxies (diamonds). Each column shows the fits for a given model, following the assumptions in Sec. 3.3. The top row is for the stellar Tully-Fisher relation, the middle row is for the size-velocity relation, while the bottom row is for the angular momentum-velocity relation. The white filled points in the plots are the galaxies which do not satisfy the Lelli et al. (2016b) criterion on the flatness of their rotation curves. The yellow filled points in the $j_* - V_{flat}$ relation are the 92 SPARC galaxies with 'onverged j_* profiles, following Posti et al. (2018a).

В массивных спиралях – «космическое» отношение звезд и темной материи:

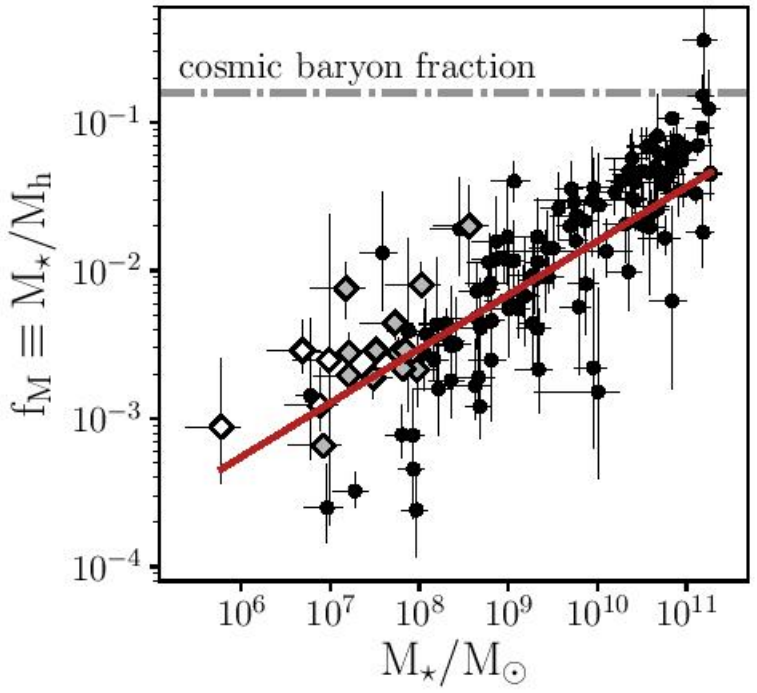

Fig. 4. Global star formation efficiency $f_M \equiv M_\star/M_h$ as a function of $M_\star$ for the SPARC and LITTLE THINGS galaxies. The measurements of the halo masses come from PFM19 and Read et al. (2017), respectively. Symbols are the same as in Fig. 2. The red line indicates the $f_M - M_\star$ relation derived in the linear model for guidance.

Как в линейной модели

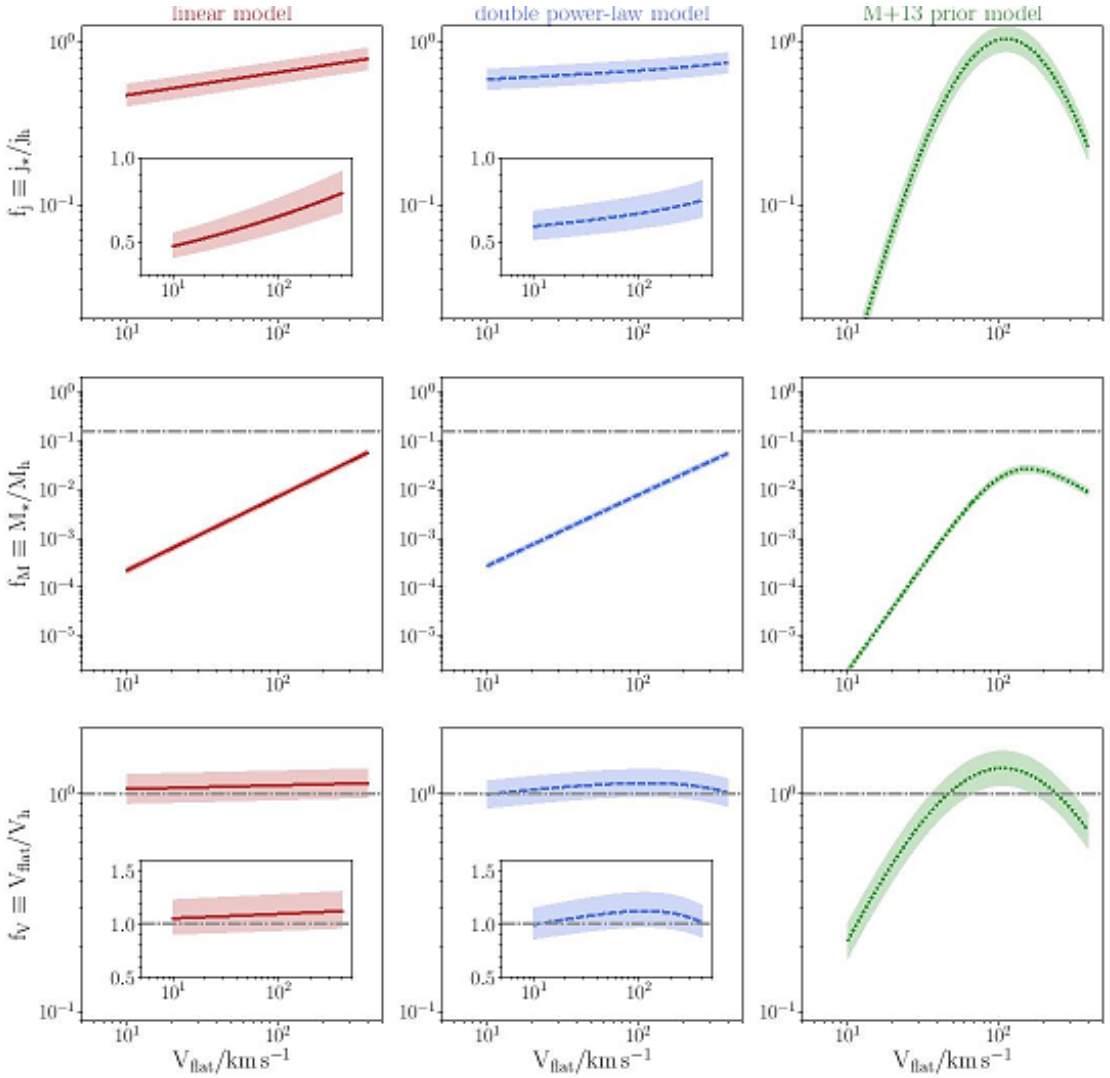

Fig. 3. Model predictions. We show how f_j (top row), f_M (middle row), and f_V (bottom rows) vary as a function of V_{flat} for the three best models (columns). In the middle row the dot-dashed line shows the value of the cosmic baryon fraction $f_b = 0.157$, while in the bottom row the dot-dashed line indicates the value $f_V = 1$. The insets show a zoom-in of the plots in linear scale.

Abundance matching никак не годится!

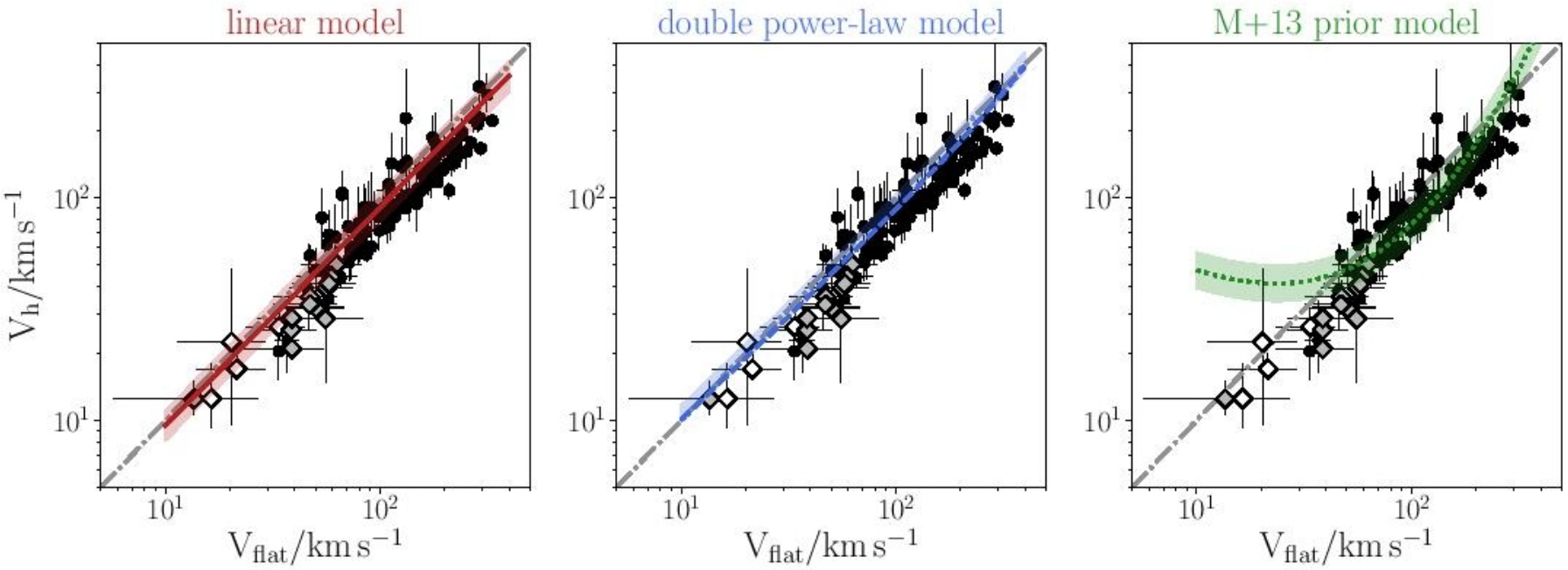

Fig. 5. Comparison of the predictions of the three models in the $V_{flat} - V_h$ plane, with data for the SPARC (circles) and LITTLE THINGS galaxies (diamonds). The halo virial velocities have been obtained with a careful rotation curve decomposition by Read et al. (2017) for the LITTLE THINGS galaxies and by PFM19 for the SPARC galaxies. In all panels, the grey dot-dashed line is the 1:1 and the symbols are the same as in Fig. 2.

ArXiv: 1909.01230

Gas accretion as fuel for residual star formation in Galaxy Zoo elliptical galaxies

Timothy A. Davis[1]★ and Lisa M. Young[2,3]

[1]*School of Physics & Astronomy, Cardiff University, Queens Buildings, The Parade, Cardiff, CF24 3AA, UK*
[2]*Physics Department, New Mexico Tech, 801 Leroy Place, Socorro, NM 87801, USA*
[3]*Adjunct Astronomer, National Radio Astronomy Observatory, Socorro, NM 87801, USA*

Accepted 2019 September 3. Received 2019 August 20; in original form 2019 July 11.

ABSTRACT

In this letter we construct a large sample of early-type galaxies with measured gas-phase metallicities from the Sloan Digital Sky Survey and Galaxy Zoo in order to investigate the origin of the gas that fuels their residual star formation. We use this sample to show that star forming elliptical galaxies have a substantially different gas-phase metallicity distribution from spiral galaxies, with ≈7.4% having a very low gas-phase metallicity for their mass. These systems typically have fewer metals in the gas phase than they do in their stellar photospheres, which strongly suggests that the material fuelling their recent star formation was accreted from an external source. We use a chemical evolution model to show that the enrichment timescale for low-metallicity gas is very short, and thus that cosmological accretion and minor mergers are likely to supply the gas in $\gtrsim 37\%$ of star-forming ETGs, in good agreement with estimates derived from other independent techniques.

Выборка

For an object to be classified as an elliptical at least 80% of Galaxy Zoo users must have placed it in this class. A statistical de-biasing correction is included (as discussed in Bamford et al. 2009).

Matching these catalogues leaves us with a total sample of 662,888 objects, of which 61,911 are classified as elliptical galaxies. Of these 61,911 elliptical galaxies 567 (0.92%) have stellar masses above 5×10^9 $M_\odot$, and measurable gas-phase metallicities (i.e. the ratios of their ionised gas lines are consistent with ionisation from star-formation, based on the criteria of Kauffmann et al. 2003b). These are the objects we will study further in this work.

This sample contains ETGs with stellar masses from 5×10^9 – 7×10^{12} $M_\odot$, with redshifts from 0.014 – 0.30 (although we note that 65% of our sample is at $z < 0.1$, likely because of the difficulty in classifying high-redshift objects in SDSS imaging). The lowest SFR probed in our sample is 0.03 $M_\odot$ yr^{-1}, and the median is 2 $M_\odot$ yr^{-1}. These objects are found throughout the u-r colour magnitude diagram, however 3/4 of the sample are bluer than expected for red-sequence objects at this redshift (with $u - r$ colours < 2.4), and thus our sample likely has significant overlap with the smaller sample of 204 blue ETGs selected from Galaxy Zoo by Schawinski et al. (2009).

Выбрали 42 E-галактики с обедненным газом

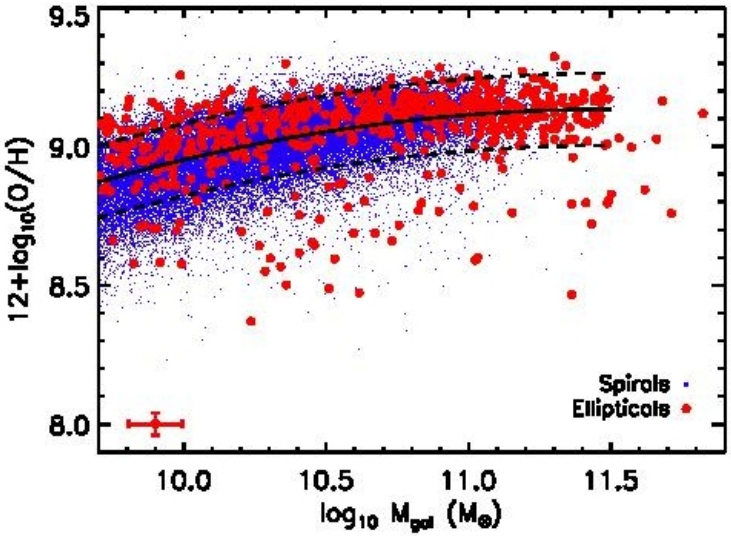

Figure 1. Gas-phase metallicity plotted vs stellar mass for Galaxy Zoo classified spiral (blue dots) and elliptical galaxies (red points). The median error for the ETG points is shown in the bottom left corner. The mass – metallicity relation of Tremonti et al. (2004) is shown as a solid black line, with its 1σ scatter shown as dashed lines. A significant population of low gas-phase metallicity ellipticals are found well below the mass – metallicity relation.

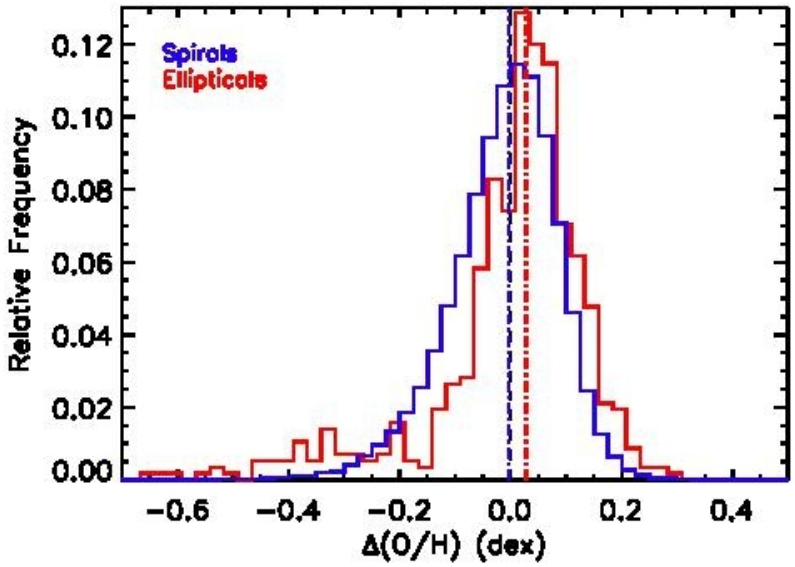

Figure 2. Histogram of the residuals around the mass – metallicity relation of Tremonti et al. (2004) for Galaxy Zoo classified spiral (blue) and elliptical galaxies (red). The black dashed line shows an offset of zero as a guide to the eye, while the blue and red dash-dot lines show the median of the spiral and elliptical galaxy populations, respectively. The average star forming elliptical galaxy is slightly more metal rich than the average star forming spiral galaxy (at fixed mass), but a tail of very low metallicity galaxies also exists, which is significantly more prominent for ellipticals than spirals.

У них у всех звезды намного более металличные, чем газ

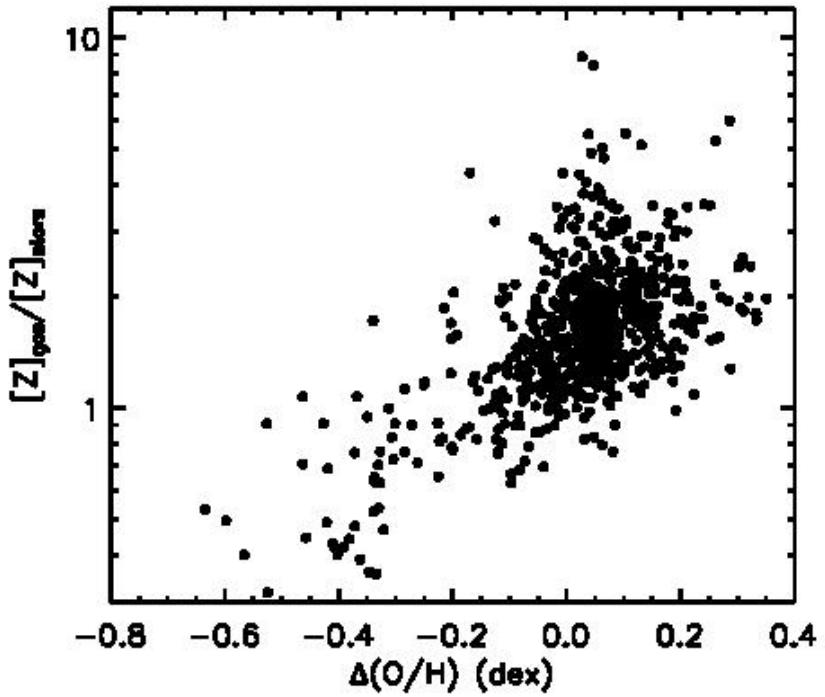

Figure 3. Residuals around the mass – metallicity relation of Tremonti et al. (2004) for Galaxy Zoo classified elliptical galaxies, plotted against the ratio between the gas-phase and stellar metallicities for each object (where each of these metallicities is expressed in solar units, with an assumed oxygen metallicity of the sun of 12+log(O/H)=8.9; Anders & Grevesse 1989). The elliptical galaxies which lie well below the mass – metallicity relation typical have lower gas-phase than stellar metallicity, a clear signature that this material is not provided by stellar mass loss.

Примитивная модель химической эволюции говорит, что это весьма НЕДАВНЯЯ аккреция

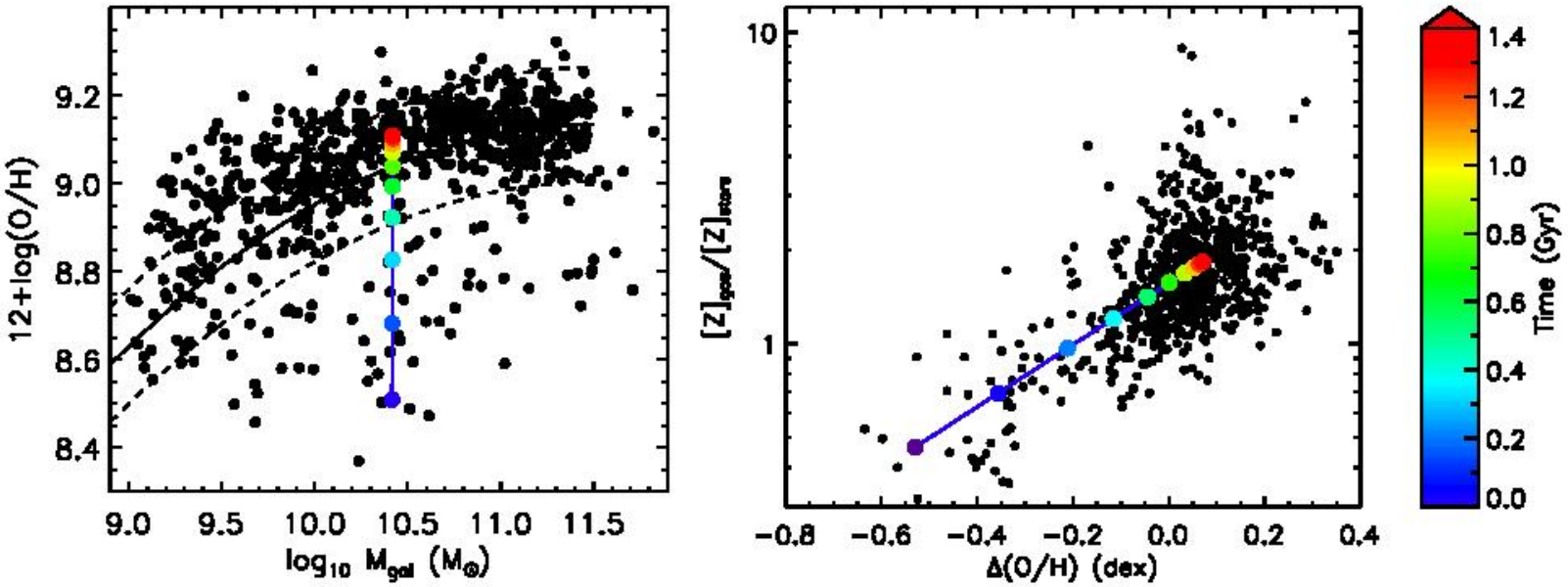

Figure 4. Mass vs metallicity (left-hand panel) and residual metallicity vs enhancement of the gas-phase metallicity (right-hand panel), as in Figures 1 and 3. The blue lines show the track followed by a typical galaxy from our observational sample (with a stellar mass of 2.6×10^{10} $M_\odot$ and a stellar metallicity of 0.89 $Z_\odot$) as it undergoes a burst of star caused by 5×10^{8} $M_\odot$ of cold gas which initially has a metallicity of 0.1 $Z_\odot$. Coloured points along this line, and the colour-bar on the far right, show how quickly our model galaxy moves in this space. The signature of metal-poor accretion is only visible for ≈400 Myr.